Chemical Engineering and Processing 78 (2014) 1–10

Contents lists available at ScienceDirect

Chemical Engineering and Processing: Process Intensification

journal homepage: www.elsevier.com/locate/cep

Computational study of the effect of processing parameters on the formation and growth of ZrO_2 nanoparticles in FSP process

Hosein Torabmostaedi, Tao Zhang*

Faculty of Science, Engineering and Computing, Kingston University, London SW15 3DW, UK

ARTICLE INFO

Article history:
Received 13 July 2013
Received in revised form 2 January 2014
Accepted 24 January 2014
Available online 1 February 2014

Keywords:
Nanoparticle
Flame spray pyrolysis
Controlled scale-up
Computer simulation

ABSTRACT

Flame spray pyrolysis (FSP) offers a proven and inexpensive route for nanoparticle production. To date, the research on FSP made nanoparticles was focused mostly on the lab scale and medium scale production. Scale-up requirements for FSP process control need to be developed to define the operation window at industrial scale production rate. In this work, FSP synthesis of ZrO_2 particles has been addressed from a process intensification perspective, since FSP characteristics perfectly fit into several fundamental process intensification aspects. The possible solutions for the precursor delivery system and the atomization quality at high precursor concentrations were investigated to intensify the production rate and reduce the cost of an additional solvent. The simulation results showed that the particle size could be controlled at near a constant (~20 nm) while the production rate was intensified by a factor of 5. Finally, the potential of gas to liquid flow ratio (GLFR) and replacing oxygen dispersion gas by air for further reducing the particle size and the production cost were investigated. The simulation results can be used as a framework of PI in FSP process design at industrial scale production.

1. Introduction

One of the most important problems for the extensive usage of nanoparticles in industry is the complexity in producing particles with high purity and desirable phase and morphology. This challenge is further increased in large-scale production where it is necessary to keep the cost at minimum. Flame spray pyrolysis (FSP) offers a versatile technology to produce metal-oxide particles, typically with 10–100 nm diameter. An apparent benefit of FSP to gas-fuelled processes is to use both organic and inorganic precursors to produce nanoparticles and it has the advantage of dissolving precursor directly in the fuel [1]. In addition, FSP reactors are normally designed with a convergent–divergent nozzle, which gives a superior acceleration to the gas flow and high momentum output to the powder particles. Research on the range of materials that can be produced by flame synthesis has shown that FSP generates more accessible product compounds than gas-fuelled systems as they are not reliant on highly volatile precursor compounds [2].

In FSP process, premixed fuel and precursor are atomized by using a gas-assisted nozzle. The atomized solution is ignited by using a small pilot flame which is positioned around the nozzle tip. The energy of the flame is used to drive chemical reaction of the precursor to produce clusters which quickly grow into nanoparticles by coagulation and sintering. The characteristics of the primary and agglomerate particles depend on the precursor concentration, temperature and velocity profile and residence time of particles in high temperature zone. Unfortunately, these parameters cannot be changed independently and any change in one parameter would affect the others. The overall process includes atomization, evaporation, combustion, supersonic flow expansion, turbulent mixing and liquid–gas–solid interaction which increase the complexity for the process control. As a critical element of the process, combustion provides the required energy for decomposition of precursor and also affects the growth of particles after decomposition. An efficient combustion process is very important to produce particles with high chemical purity and desirable phase and morphology.

To date the research on FSP has progressed in both experimental [3,4] and modelling fashions [5,6]. Experiments were mostly focused on lab scale [1,7,8] and medium scale productions [3,4,9–11] while the industrial scale requirements have never been investigated. Several parameters need to be studied and optimized in order to have a controlled synthesis at industrial scale production rate. Since measuring the profile of the flame and the characteristics of the products during the process is expensive, time consuming and impossible for some parameters, numerical modelling was found to be an excellent tool for optimizing the FSP process.

Over the last two decades, several semi-empirical models have been developed to provide insight to the formation and growth of particles in flames [12–14]. Among these models, the

* Corresponding author. Tel.: +44 208 5478103; fax: +44 208 5478103.
E-mail address: t.zhang@kingston.ac.uk (T. Zhang).

0255-2701/$ – see front matter © 2014 Elsevier B.V. All rights reserved.
http://dx.doi.org/10.1016/j.cep.2014.01.009

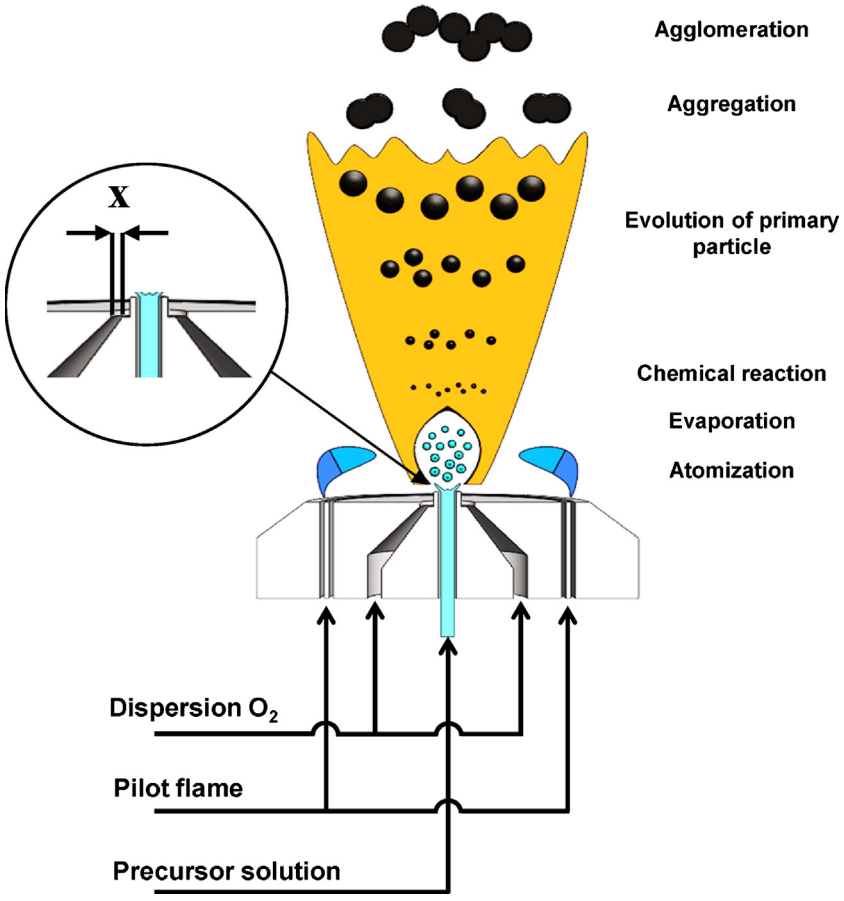

Fig. 1. Schematic view of FSP nozzle configuration.

monodisperse model of Kruis et al. [13] was applied to many studies [3,15–17] due to its simplicity and a superior performance for predicting the final particle size. Torabmostaedi et al. [6] studied the effect of processing parameters on the flame structure and the characteristics of particles at medium scale production rates. A commercial CFD code, FLUENT was used to solve the multi-component droplet evaporation, combustion and the gas flow field in FSP.

The CFD code was coupled with an in-house Fortran code which was based on the model developed by Kruis et al. [13] to simulate the particle growth during FSP. The employed mathematical models were tested against the experimental data. The prediction for gas dynamics, initial droplet size and primary particle diameter in FSP process was validated against the documented experimental measurements [3,4,11]. It was shown that the primary particle size can be closely controlled at 15.5 nm in medium production rates by creating a constant residence time for zirconia nanoparticles at high temperature zone through a constant gas to liquid flow ratio (GLFR) at a low precursor concentration (0.5 M ZnP in ethanol). To achieve high production rate the precursor concentration has to be increased. However, the results in previous study [6] has shown that at higher precursor concentration, the primary particle size was significantly increased since the higher particle concentration increased the coagulation and therefore enhanced the growth of primary particles above the burner [6]. In addition, it is a challenge to scale up the production rate due to the limitation of precursor delivery system and atomization quality which are influenced by the physical properties of precursor solutions at higher precursor concentrations.

The main aspect of process intensification (PI) lies in the development of new techniques which offer drastic improvement in the efficiency of the manufacturing, substantially decreasing the equipment operating cost and delivering a safer process [18]. From this perspective, the following modifications in the process parameters of FSP are proposed as a solution to address the fundamental aspects of PI:

(i) Delivering the highest possible precursor concentration to the nozzle.
(ii) Increasing the precursor volumetric flow rate.
(iii) Using air as oxidant/dispersion gas.

Increasing the precursor concentration lowers the cost of additional solvent while intensifying the production rate. Moreover, running a single FSP burner at a higher precursor volumetric flow rate intensifies the nanoparticle production rate while reducing the operation cost. And finally, replacing oxygen with air as the dispersion gas would result in huge saving for the oxidant cost at the industrial scale production rates. In addition, the process safety will be increased when air was used as the dispersion gas since extra nitrogen needs to be heated up which lowers the flame temperature.

However to implement these ideas in the experimental setup, optimization studies are needed to create an operation window for the synthesis of nanoparticles in an industrial scale. This work investigates the processing requirements needed to increase the efficiency of the nanoparticle production in FSP, reduce the operation cost and create a safer process to fulfil all fundamental aspects of PI defined by Stankiewicz and Moulijn [18]. Zirconia is studied here due to its unique thermal and

mechanical properties and its wide-spread applications in industry [19–21].

2. Model development

2.1. Computational fluid dynamics

The FSP system used in this study is schematically shown in Fig. 1. The configuration of the burner is consistent with the one studied by Torabmostaedi et al. in previous investigation [6] but without the additional sheath gas. The nozzle consists of a capillary tube (0.5 or 0.8 mm) for feeding the precursor solution and an annular gap x for the exit of oxidant/dispersion gas (x is the width of the gap, see Fig. 1) for atomizing the precursor solution. The annular gap size affects the pressure drop in the working mass flow rate. There are two concentric openings (9/9.5 and 10/12.5 mm in ID/OD) around the atomizing gas inlet. Methane and oxygen were supplied through these two annuli to form a diffusion flame to ignite the main flame. The solutions of zirconium n-propoxide 70 wt% in n-propanol diluted in ethanol at 1, 1.5, and 2 M concentration are injected into a pre-existing methane–oxygen flame. The solvent(s) evaporates and combusts to form a high temperature flame. At that stage, chemical reactions and particle growth will take place to produce nanoparticles.

The computational geometry for the burner, external domain, grid structure and boundary conditions were fully described in the previous study [6] and hence only a brief description is given in this paper. A structured grid is used and fine meshes are employed to the inlet/exit of the dispersion gas where high gradients are expected so that high accuracy is required in order to capture the compressibility effects. The modelling of gas dynamics, droplet transport, turbulent, chemical reaction and radiation were fully described by Torabmostaedi et al. [6]. A comparison between prediction models of viscosity and surface tension [22–24] with experiments [6] showed that the models provided by Hind et al. [24] and Tamura and Kurata [23] had a good match with tested results and these models were selected in this study to predict the viscosity and surface tension.

2.2. Particle dynamics

The CFD code was coupled with an in-house Fortran code which was developed based on the Kruis et al. [13] model to simulate the particle growth during FSP. The growing rate of the initial zirconia particles is controlled by coagulation and sintering. The expressions for the surface area of a completely fused (spherical) aggregate a_s and the collision frequency function β can be found in Kruis et al. [13]. The fractal dimension, D_f, was set as 1.8, a commonly used value for aggregates generated in high temperature aerosol processes [13,25]. The dynamics of particle growth have been fully described in the previous work by Torabmostaedi et al. [6].

3. Results and discussion

3.1. Effect of physical properties of precursor solution

The fuel spray characteristics have a great influence on the performance of FSP process. Any change in the physical properties of the liquid solution will change the spray characteristics of a fuel injection. The significant properties of the liquid materials are (in order of significance): viscosity, surface tension and density [26]. High viscosity and surface tension increase the amount of energy required to atomize the spray. An increase in any of these properties will increase the droplet size. The following two parameters, commonly encountered in FSP, are directly affected by liquid physical properties:

- Pump pressure requirement.
- Atomization quality and evaporation.

Viscosity is an important factor which affects the performance of the pump used in the system. Prior to designing a pump for industrial scale production, it is important to determine the effects of viscosity of the fluid at the expected operating conditions. An increase in liquid viscosity generally increases the required net inlet pressure and the required pump input power. Increasing the viscosity and surface tension tends to increase the size of the droplets, which in turn decreases the acceleration of the flame. The effect of liquid density on the initial droplet size is relatively small but complex [27]. Moreover, Miesse's experimental results [28] revealed that the effects of flow conditions and physical properties on the maximum droplet diameter depend on the liquid Reynolds number. For example, an increase in liquid density decreases the droplet diameter when $Re_L < 29{,}750$, but increases it at larger Reynolds number. The effect of liquid properties should be understood and accounted for when selecting the process operations.

In FSP, it is very important to maintain the viscosity and surface tension of solution at a low level to achieve satisfactory droplet distribution and evaporation rate at applied pump pressure. For precursor solutions, this minimum viscosity and surface tension may only exist over a very narrow composition range so that a very careful control may be required.

In order to control these properties at different compositions, series of mixtures were prepared at different precursor concentrations (1, 1.5, and 2 M ZnP in ethanol) and then, the viscosity and surface tension of these mixtures were measured at different operating temperatures ranging from 25 to 60 °C. Increasing the temperature of liquids tends to decrease the cohesive force while simultaneously increase the rate of molecular interchange. The former decreases the shear stress, while the latter increases it. The net result is that the viscosity of liquids will decrease with increasing temperature. Increasing the temperature also increases the kinetic energy of the molecules, and thus decreases the intermolecular attraction. This will decrease the force of surface tension. This can be clearly seen in Fig. 2.

Fig. 2 shows the average viscosity and surface tension of precursor solutions as a function of ZnP concentration at different temperatures. The average viscosities of the solutions of 1, 1.5, and 2 M ZnP in ethanol were decreased from 3.1, 7.22 and 29 mPa s to 2.6, 2.87 and 8.4 mPa s respectively when the temperature of mixture increased from 25 to 60 °C. The surface tension was also reduced as the temperature was increased. The surface tensions of the solutions of 1, 1.5, and 2 M ZnP in ethanol were decreased from 23.5, 24.8 and 25.6 mN/m to 21.2, 21.9 and 22.5 mN/m, respectively. The calculated values had the same behaviour and showed a good agreement with the measured data.

3.1.1. Pump pressure requirement

In order to scale up the nanoparticle production in FSP, several parameters need to be studied for choosing the right nozzle and pump. Increasing the production rate requires to increase the liquid flow rate and/or the precursor concentration. The latter is more efficient since operating the FSP reactor at the highest possible precursor concentration would intensify the production rate and reduces the cost of additional solvent. As shown in Table 1, the production rate was increased by a factor of 4 and solvent required was reduced by a factor of 9 when the precursor concentration was increased from 0.5 to 2 M at a constant feeding rate of solutions. However it has the disadvantage of high viscosities which requires raising the pumping pressure. The smaller the size of the nozzle orifice, the greater the pumping pressure is needed to pump liquid through the nozzle. Therefore, studies have been carried out to investigate these effects and the data will be used for the design of

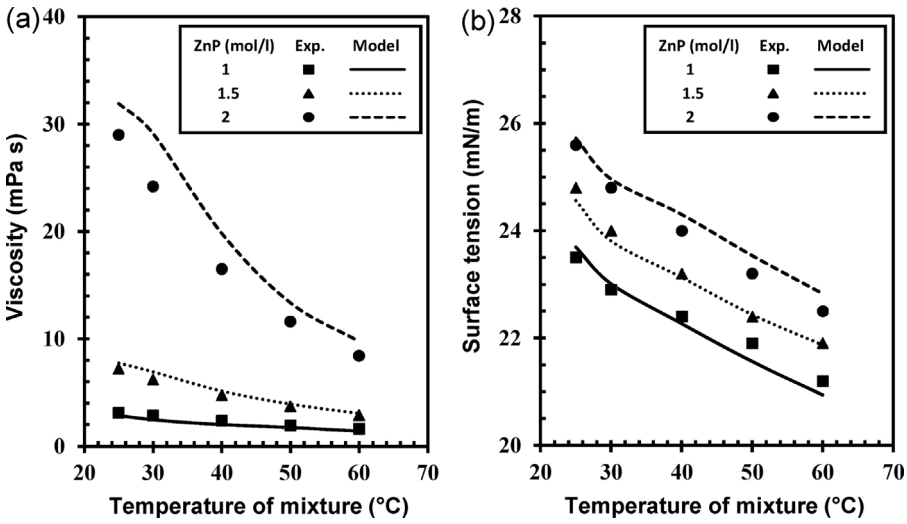

Fig. 2. Comparison of measured (symbols) and calculated (lines) (a) viscosity and (b) surface tension of precursor solutions as a function of temperature.

a required nozzle and pump in industrial scale production. When the Reynolds number $Re < 2300$, the flow in the nozzle is laminar and the liquid flow rate can be represented by the well-known Hagen–Poiseuille equation [29]

$$Q = \frac{\Delta P \pi d^4}{128 \mu l} \quad (1)$$

When the Reynolds number $Re > 2300$, the flow in a nozzle may become turbulent, and the liquid flow rate at low turbulent numbers can be represented as

$$Q = \left(\frac{\Delta P}{0.241 l \rho^{3/4} \mu^{1/4} d^{-4.75}} \right)^{1/1.75} \quad (2)$$

Here μ and ρ are the viscosity and density, ΔP is the pressure drop, over the length l of the nozzle orifice with size d. The length, l, was adjusted for different nozzle orifice to validate the measured flow rates (data supplied by Düsen–Schlick GmbH). In both laminar and turbulent flows, the flow rate can be increased by increasing the applied pressure and the size of the nozzle orifice and can be reduced by increasing the viscosity of the mixture and the length of the nozzle. In order to check the accuracies of Eqs. (1) and (2), two case studies were performed for a commercially available nozzle (Schlick two-substance nozzle, model 940) by comparing the calculated and measured water flow rates at different applied pressures. Since the pressure range data available for model 940 was limited to higher pressure range (0.1–4 bar), the lower range data was taken from different Schlick nozzle (model 930) to investigate the accuracy of the model for both laminar and turbulent regimes (see supplementary material). Water was chosen due to the availability of the experimental data from Düsen–Schlick GmbH. This nozzle was chosen for this study since it can provide the required output for the industrial production (1–5 kg/h) at medium and high precursor concentration (1, 1.5 and 2 M ZnP/ethanol).

For the calculation of water flow rate using Eqs. (1) and (2), the mass density ρ and viscosity μ were taken as 1000 kg/m^3 and 0.00114 Pa s, respectively (water at 16 °C). Fig. 3 shows the water flow rates as a function of pressure drop across the nozzle with two different orifice sizes. The predicted data are compared with measured flow rate using Eq. (1) for laminar (thick lines) and Eq. (2) for turbulent flows (thin lines). In laminar region (d (0.5 mm): $Q < 60$ ml/min; d (0.8 mm): $Q < 100$ ml/min), the flow rate increases linearly with pressure drop for both orifice sizes. This is due to the direct relationship between the flow rate and pressure drop in laminar flow as shown in Eq. (1). As the Reynolds number increased ($Re > 2300$), the flow became turbulent and nonlinear. At higher Reynolds number turbulent flow forms vortices and leads to large fluid drag which increases the pressure drop even much higher than that in the laminar case.

Increasing the applied pressure from 0.01 to 4 bar increased the water flow rate from 15 to 330 ml/min for the orifice with 0.5 mm diameter while the flow rate increased from 40 to 840 ml/min for the orifice with 0.8 mm diameter. While keeping the applied pressure and viscosity constant (viscosity is constant since all the measurements were performed with water at 16 °C), increasing the orifice diameter from 0.5 to 0.8 mm increased the water flow rate by a factor of 2.5. The model showed a good agreement with the measured data and therefore it can be used for the design of FSP nozzle and the modification of the physical properties of precursor

Table 1
Effect of precursor concentration on the process efficiency and production cost.

ZnP concentration (M)	0.5	1	1.5	2
ZnP/ethanol feed rate (ml/min)			67.5	
ZrO_2 production rate (g/h)	250	500	750	1000
Ethanol dilution in ZnP (wt%)	72	48	27	8

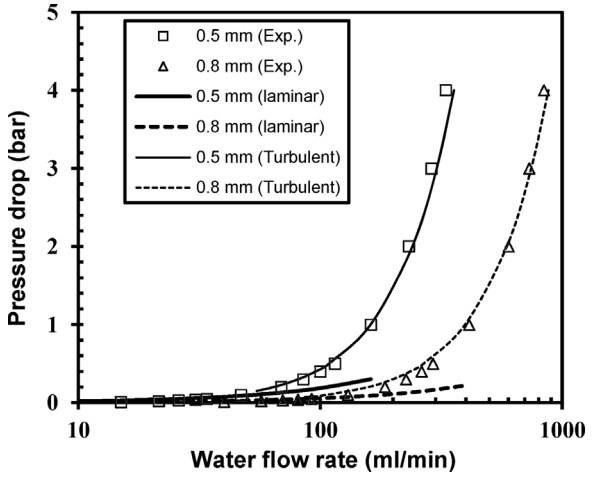

Fig. 3. Water flow rate as a function of pressure drop across the nozzle tip using different nozzle orifice sizes. The measured data are compared with predicted data obtained using Eqs. (1) and (2) for laminar (thick lines) and turbulent flows (thin lines).

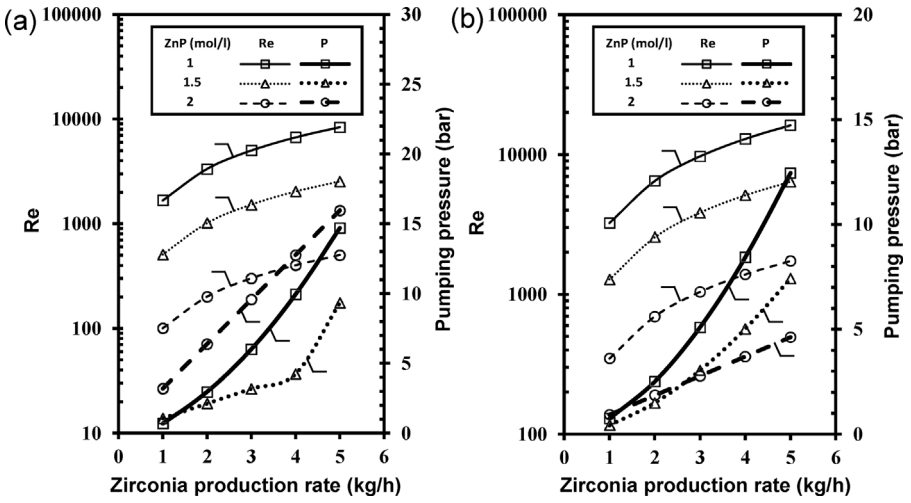

Fig. 4. Pumping pressure and *Re* as a function of production rate and ZnP concentration for the 0.5 mm nozzle at precursor solution temperatures; (a) 25 °C and (b) 60 °C.

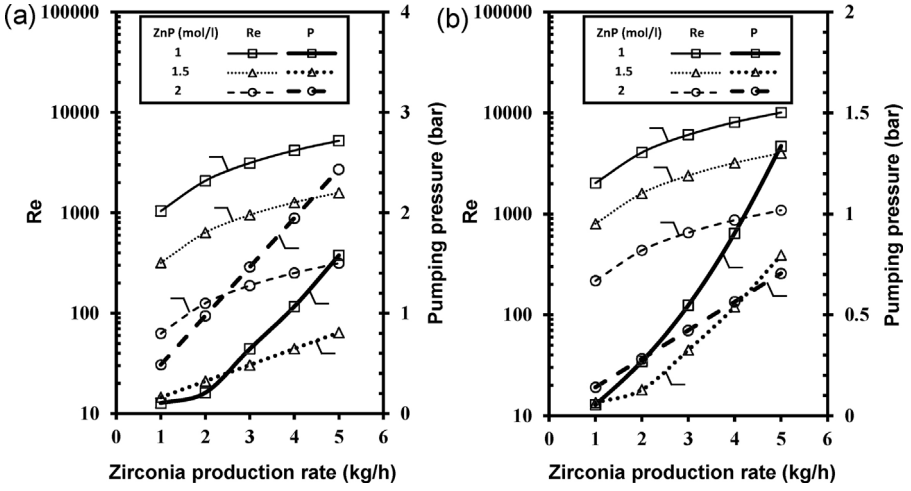

Fig. 5. Pumping pressure and *Re* as a function of production rate and ZnP concentration for the 0.8 mm nozzle at precursor solution temperatures; (a) 25 °C and (b) 60 °C.

solutions to reduce the pumping pressures required at industrial scale production rates.

Figs. 4 and 5 show the predicted flow rates and Reynolds numbers as a function of pressure drop for 1, 1.5 and 2 M ZnP/ethanol solutions at the production rates of 1–5 kg/h zirconia using two different liquid mixture temperatures (25 and 60 °C) and nozzle orifice sizes (0.5 and 0.8 mm). To calculate the flow rate of ZnP/ethanol at different concentrations of ZnP using Eqs. (1) and (2), the viscosity μ was adopted from Fig. 2a while the density was calculated using the following equation:

$$\rho_{mix} = \frac{1}{\sum_{i=1}^{n}(Y_i/\rho_{l_i})} \quad (3)$$

where Y_i and ρ_{l_i} are the mass faction and density of component i, respectively.

Fig. 4a shows that the pumping pressure increases when the zirconia production rate is increased. For the 1 and 1.5 M ZnP/ethanol solutions, the flow became turbulent at just below 2 and 5 kg/h zirconia production, respectively. This can be seen from the values of Reynolds number at these production rates which results in a sharp increase on the required pumping pressure due to the formation of vortices at higher Reynolds number. At higher ZnP concentration (2 M ZnP/ethanol), the flow was laminar even for the production rate over 5 kg/h. This is due to the higher viscosity of the liquid solution at higher precursor concentration. Increasing the ZnP concentration from 1.5 to 2 M increased the pumping pressure by a factor of 1.7 at 5 kg/h production rate.

Fig. 4b shows the effect of ZnP/ethanol temperature while the same nozzle orifice and production rates as described in Fig. 4a were used. Increasing the mixture temperature reduced the viscosity of the solution (see Fig. 2a), thus, lowered the pressure drop especially at higher ZnP concentration (2 M ZnP/ethanol). The flow was nearly turbulent for the whole production range for 1 M and 1.5 M ZnP/ethanol while it was still laminar for 2 M ZnP/ethanol solution. Increasing the temperature from 25 to 60 °C was not effective enough to change the flow regime but was effective on reducing the pressure drop (due to lower viscosity). The pressure drop was decreased by a factor of 3.45 at 2 M ZnP/ethanol when the temperature was increased from 25 to 60 °C. Another factor which can help to reduce the pumping pressure more effectively than temperature is the nozzle orifice. Fig. 5a shows the predicted flow rates and Reynolds numbers of 1, 1.5 and 2 M ZnP/ethanol solutions at 25 °C for the production of zirconia at 1–5 kg/h as a function of pressure drop using nozzle orifice size of 0.8 mm.

Increasing the orifice size by keeping the zirconia production rate and mixture temperature constant reduced the mixture velocity and consequently the Reynolds number and pressure drop. The pumping pressure was reduced by a factor of 6.5 at 2 M ZnP/ethanol as the orifice size increased from 0.5 to 0.8 mm. Fig. 5b shows the effect of ZnP/ethanol temperature for the same nozzle orifice and

production rates as described in Fig. 5a. Increasing the mixture temperature for 2 M ZnP/ethanol solution decreased the pumping pressure with the same factor (3.45) as was seen in the smaller nozzle orifice size (0.5 mm). Bigger orifice size and higher solution temperature were effective in reducing the required pumping pressure.

3.1.2. Initial size of ZnP/ethanol droplets

The increase of viscosity and surface tension of the precursor solutions at higher precursor concentrations affects the degree of atomization (i.e. size of the droplets). In the previous section, it was shown that increasing the temperature of precursor solution and nozzle orifice size could help to decrease the pumping pressure. It was also shown that increasing the size of orifice was more effective than increasing the solution temperature but certainly larger orifice has a negative effect on the droplet size which is one of the key factors controlling the evaporation process.

Increasing the viscosity, surface tension and nozzle orifice size tends to increase the size of the droplets, which in turn decreases the acceleration of the flame. For a given mass of liquid, smaller droplets (due to lower viscosity and surface tension) yield greater total surface area than larger droplets. Greater surface area provides increased contact between the continuum phase and the liquid droplets and is generally beneficial for the evaporation. The rate of evaporation depends on the size of droplets which is affected by viscosity, surface tension and nozzle orifice size.

Initial droplet size is a very important parameter in FSP and has a direct effect on the formation and growth of nanoparticles. Large droplets can even escape from the flame which may cause hollow particles [8]; therefore, good care must be taken to achieve small droplets with uniform distribution. Series of cases were defined in order to study the effect of nozzle orifice size, precursor concentration and temperature on the quality of atomization in FSP process (see Table 2).

Fig. 6a shows the predicted ZnP/ethanol droplet size as a function of temperature (25–60 °C) using 1, 1.5 and 2 M ZnP/ethanol solutions and a nozzle orifice with 0.5 mm diameter. Increasing the solution temperature from 25 to 60 °C decreased the droplet size from 36.9, 21.7 and 15.73 μm to 22.27, 14.81 and 11.93 μm for the 2, 1.5 and 1 M ZnP/ethanol solutions, respectively. Increasing the orifice size from 0.5 to 0.8 mm increased the droplet size by 22% for all concentrations (see Fig. 6b). This is because a smaller nozzle orifice leads to a higher velocity and resistance to the liquid and produces finer droplets.

Table 2
Processing parameters used to study the initial droplet size.

Cases	1	2	3
Zirconia production (kg/h)		1	
Nozzle orifice (mm)		0.5, 0.8	
GLFR		1300:1	
Pressure drop (bar)		7	
ZnP concentration (M)	1	1.5	2
Oxygen flow rate (l/min)	175.5	117	87.75
ZnP/ethanol feed rate (ml/min)	135	90	67.5

Table 3
Operating conditions at industrial scale production of zirconia.

Zirconia production (kg/h)	1	2	3	4	5
Nozzle orifice (mm)			0.5		
ZnP/ethanol temperature (°C)			60		
GLFR			1300:1		
Pressure drop (bar)			7		
ZnP concentration (M)			2		
Oxygen flow rate (l/min)	87.75	175.5	263.2	351	438.7
ZnP/ethanol feed rate (ml/min)	67.5	135	202.5	270	337.5

3.2. Effect of production rate at industrial scale

In previous study [6], it was shown that at medium production rate (≤300 g/h) and using low precursor concentration (0.5 M ZnP dissolved in ethanol) the primary particle size can be closely controlled by changing the processing parameters, but at higher precursor concentration, the primary particle size grew to over 20 nm since the higher particle concentration increased the coagulation and therefore enhanced the growth of the primary particles above the burner. In this study, the framework of previous [6] and current investigations described above were applied to industrial scale production to understand the effects of processing parameters and to develop a technique to increase the process efficiency. Series of cases were defined in order to investigate the effect of processing parameters for the production rates from 1 to 5 kg/h (see Table 3).

3.2.1. Flame structure

Increasing the production rate affects the flame structure which plays an important role on the formation of particles during FSP. Fig. 7a–c presents the flame temperature distributions, centreline temperature and velocity as a function of production rates from

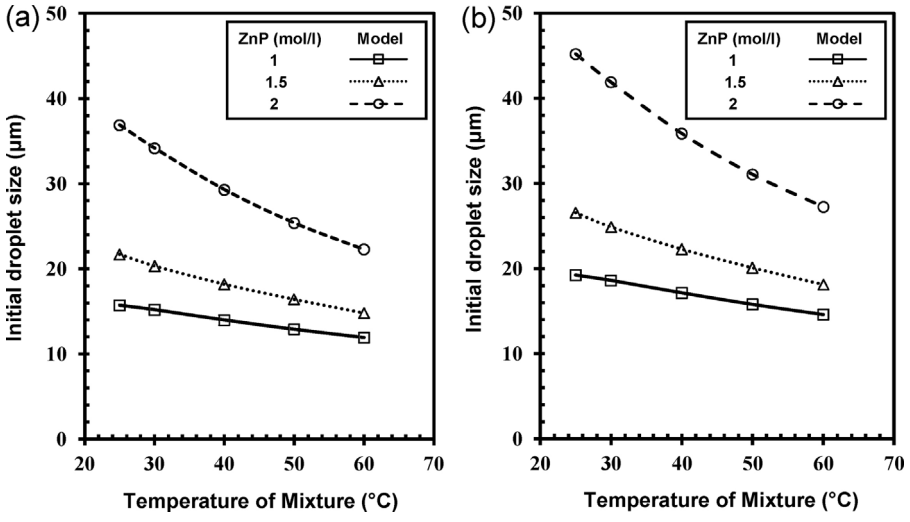

Fig. 6. The effect of precursor solution temperature on the sauter mean diameter of ZnP/ethanol droplets at orifice sizes; (a) 0.5 mm and (b) 0.8 mm.

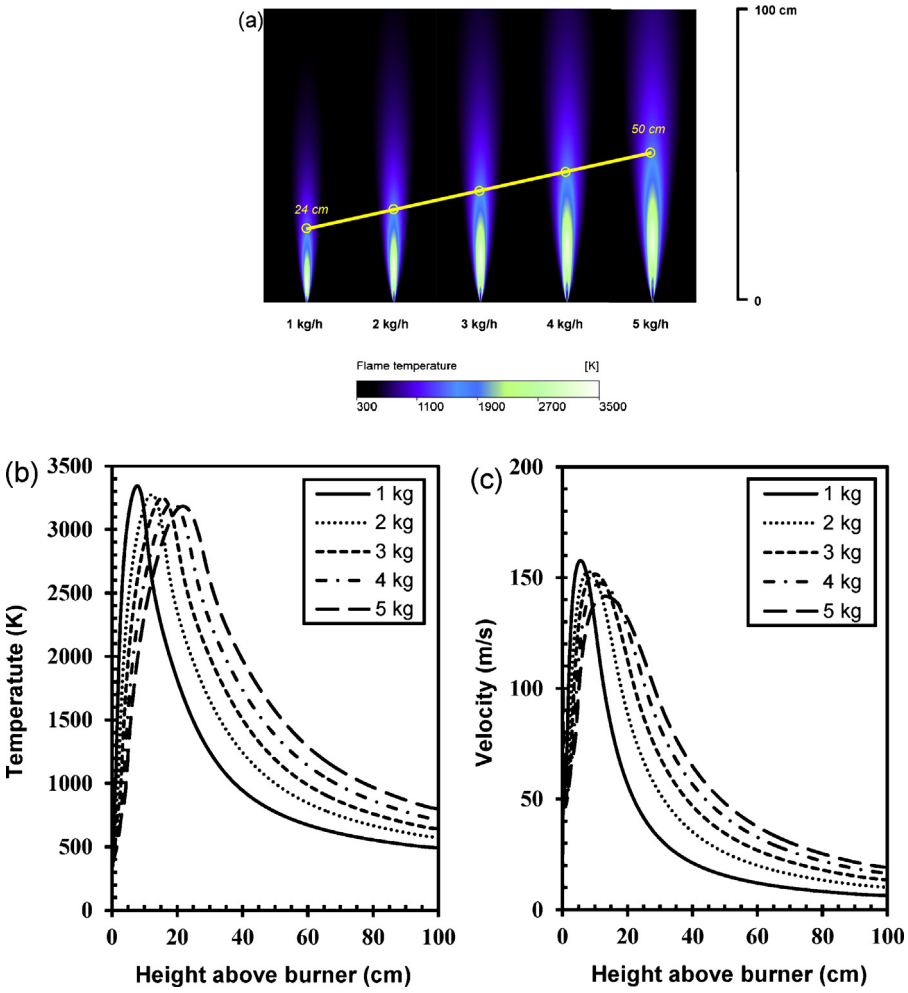

Fig. 7. Simulated (a) temperature distribution contours, and centre axis (b) temperature and (c) gas velocity profiles for the production of zirconia at 1–5 kg/h. Keeping pressure drop and GLFR at 7 bar and 1300 and ZnP concentration at 2 M.

1 to 5 kg/h. The precursor concentration was kept constant at 2 M ZnP in ethanol, the pressure drop in the nozzle was kept at 7 bar to the dispersion gas, and the GLFR was kept at 1300. It can be seen that the higher production rates led to a longer flame and bigger flame region. The spray flame height increased from 24 to 50 cm as the production rate increased from 1 to 5 kg/h. This is due to the higher supplied fuel energy which prolongs the time for the fuel combustion resulting in longer flame. Since the pressure drop and GLFR were kept constant, the value of centreline peak flame velocity is similar for all production rates but the position of the peak point above the burner is slightly higher for higher production rates. This is because the higher ZnP/ethanol feeding rate delays the evaporation and expansion of gas volume after combustion.

3.2.2. *Precursor conversion and particle size*

Fig. 8a presents the conversion of precursor ZnP above the burner along the centreline for different zirconia production rates. As the production rate increased from 1 to 5 kg/h, 100% conversion of precursor delayed nearly 20 cm above the burner which in principle may delay the formation and later on the growth of the primary particles. Fig. 8b shows that the particle size of the product is nearly constant at different production rates. The primary particle diameter was kept at ~20 nm, while the production rate was increased from 1 to 5 kg/h. This is a very important feature for scaling-up to industrial production rate. It was found that the behaviour of FSP flames in industrial-scale is the same as in medium production rate in previous study [6].

3.3. *Effect of GLFR*

The simulation studies in Section 3.2 presented an important feature for scaling-up to industrial production rate. In this section, the effect of production rate was studied for industrial-scale production at higher precursor concentration (2 M ZnP in ethanol). It was found that the particle size can be closely controlled by keeping the GLFR and pressure drop constant even at high production rates. Up to now, the simulation results showed that by keeping the GLFR constant at 1300 similar particle size of 20 nm can be obtained at fixed precursor concentration. However, to achieve a better performance, finer particles may be required and further study is needed. In order to have a controlled synthesis of zirconia particles at industrial-scale production and different particle sizes, series of cases were defined to study the effect of GLFR at different precursor concentrations.

Fig. 9 presents the effect of GLFR on the size of primary zirconia particles at precursor concentration of 1, 1.5 and 2 M ZnP in ethanol for the production of zirconia at 5 kg/h. Increasing the GLFR from 1300 to 2100 decreased the zirconia diameter from 17, 18.8 and 20.3 nm to 12.2, 13.4 and 14.6 nm for the 1, 1.5 and 2 M ZnP in ethanol, respectively. The results in this section can be very useful

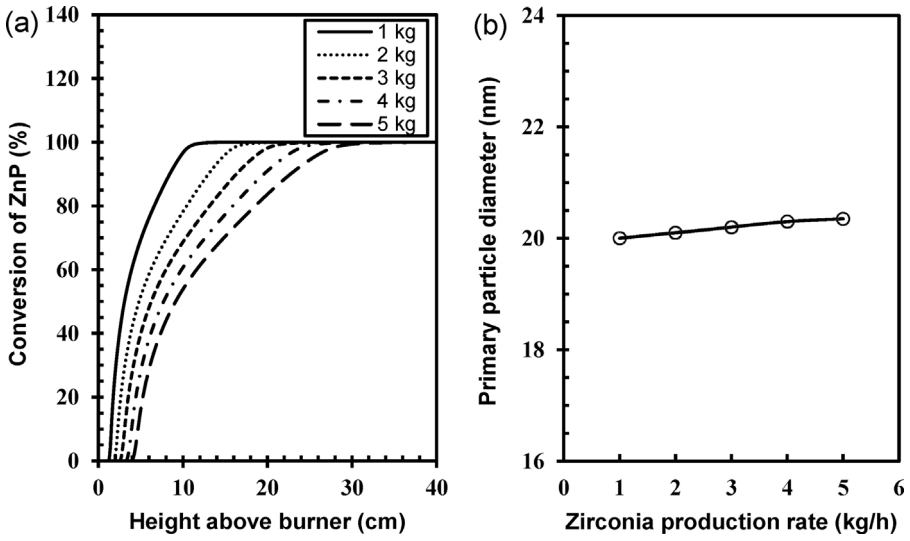

Fig. 8. Predicted (a) centre axis ZnP conversion and (b) zirconia particle size at different production rates (1–5 kg/h) by keeping the pressure drop and GLFR constant at 7 bar and 1300, respectively.

for the selection of process window for industrial-scale production of nanoparticles.

3.4. Effect of oxidant composition

The oxidant/dispersion gas composition may also affect the product quality and process efficiency. For example, using air (23% oxygen) instead of pure oxygen lowers the flame temperatures above the burner which may be able to reduce the particle size and increase the reactor's safety. In addition, using air as a dispersion gas is more economic especially at industrial scale production but it may also result in incomplete combustion. The latter would result in incomplete decomposition of precursor and consequently lower nanoparticle production rate. Mueller et al. [9] used air as dispersion gas for the production of 100–300 g/h silica. Observing the flame appearance, they concluded that replacing oxygen with air resulted in incomplete combustion at production rates above 100 g/h. This was due to the low air to fuel ratio at higher production rates (i.e. the oxidant flow rate was kept constant and solution feed rate was increased). In this section, the effect of air or oxygen dispersion gas on flame structure, particle production rate and particle size in FSP process is investigated using 2 M ZnP in ethanol by keeping the GLFR constant at 2100. In order to observe the effect of dispersion gas on the completion of combustion and the production yield of nanoparticles, the production rate Q of zirconia at 100 cm above the burner is computed by summing the value of the zirconia mass fraction multiplied by the density and the dot product of the facet area vector and the facet velocity vector.

$$Q = \sum_{i=1}^{n} Y_i \rho_i \vec{v}_i \cdot \vec{A}_i \quad (4)$$

where Y is the mass fraction of zirconia, ρ and v are the continuum phase density and velocity, and A is the area. Two cases were defined in order to study the effect of oxygen content in the dispersion gas (from 23% to 100%, see Table 4). Fig. 10a and b shows the predicted flame temperature field and production rate of zirconia at 5 kg/h using oxygen and air as dispersion gas. It can be clearly seen that the high temperature zone of the flame moved away from the nozzle exit when air was used as dispersion gas. This is a direct result of lower oxygen content of supplied oxidant above the nozzle exit. But in an intensified FSP reactor, the flame mixes with the surrounding air much more intensive than that in the conventional FSP reactors [9] (i.e. due to the higher dispersion gas pressure drop and faster fuel/oxidant mixing) and more oxygen rapidly diffuses into the flame. The diffused oxygen reacts with the nonreacted fuel mixture, which rapidly decreases the mass fraction of the fuel mixture. When the combustion reaction is completed, the temperature starts to decrease continuously. This behaviour can be clearly seen in Fig. 10c. Fig. 10c shows that the complete combustion reaction with air as oxidant was delayed by only 5 cm

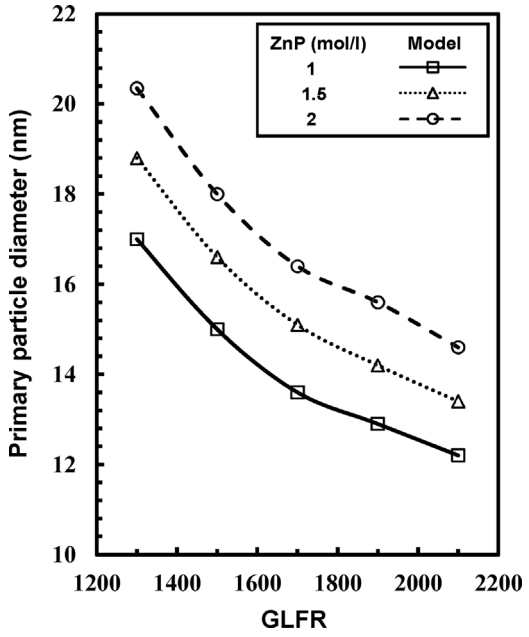

Fig. 9. Predicted primary particle diameter as a function of GLFR at different precursor concentrations for zirconia production of 5 kg/h.

Table 4
Operating conditions at different oxidant/dispersion compositions.

Zirconia production (kg/h)		5	
Oxygen content (%)	23		100
Pressure drop (bar)		7	
ZnP concentration (M)		2	
GLFR		2100:1	

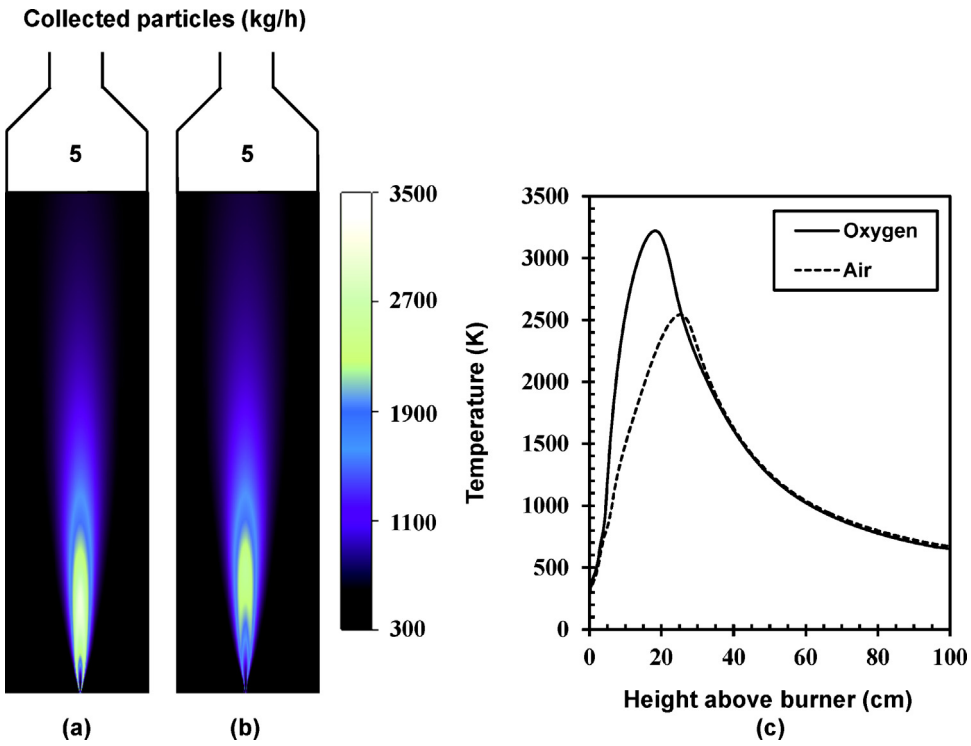

Fig. 10. Predicted temperature distribution and collected particles for the production of zirconia at 5 kg/h using (a) oxygen and (b) air with their corresponding (c) centreline temperature profiles above the burner.

when compared to that with oxygen. In order to confirm that the sufficient oxygen was available for the combustion of the precursor, Eq. (4) was used to calculate the zirconia production yield at 100 cm above the burner. In both FSP flames, the calculated collected particles at 100 cm above the burner were 5 kg/h which indicates that the combustion of the precursor was completed and the production rate was conserved.

The maximum flame temperature is also affected by the composition of dispersion gas (Fig. 10c). Using air as dispersion gas, the temperature steadily increases up to 2540 K at 25 cm above the nozzle exit. In the case of pure oxygen the temperature rises up to 3220 K at 18 cm above the nozzle exit. The maximum flame temperature is reduced by 21% since the additional nitrogen does not take part in the combustion but needs to be heated up. Since similar flame heights are achieved in both flames, slower evaporation and decomposition of precursor at lower temperatures (using air as dispersion gas) would greatly delay the formation and growth of the particles in the spray flames. This can be seen in Fig. 11, which shows the predicted evolution of zirconia primary particle and agglomerate collision diameter using air or oxygen as dispersion gas. Using air as dispersion gas, the primary and collision agglomerate diameter of product zirconia powders are decreased from 15 to 12.1 nm, and from 100 to 84 nm, respectively. This is a great feature for process optimization in FSP.

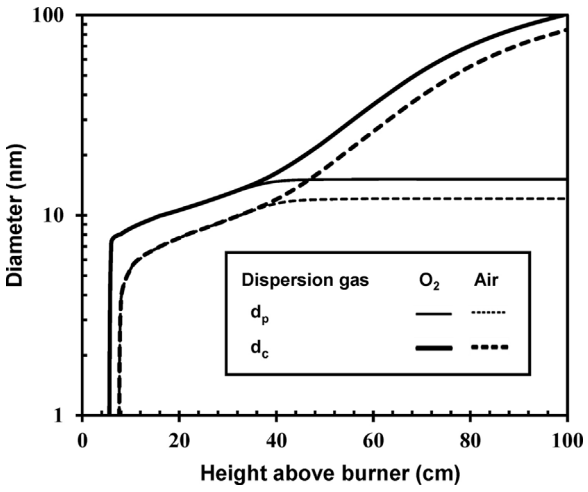

Fig. 11. Evolution of zirconia primary particle (thin lines, d_p) and agglomerate collision (thick lines, d_c) diameter using oxygen (solid lines) and air (dash lines) as dispersion gas.

4. Conclusions

The computer models developed for FSP process were used for the first time within a process intensification perspective for advanced material synthesis. The fundamental characteristics that make FSP well-fitting in the wide area of PI techniques are mainly related to the manufacturing efficiency, lower production cost, and process safety arising from reactor geometries and the processing parameters. Furthermore PI features of FSP synthesis including (a) using the highest possible precursor concentration, (b) the higher solution volumetric flow rate, and (c) the potential of using air as dispersion gas were investigated. The solution temperature, pumping pressure and the geometry of reactor were jointly investigated as a solution for delivering the highest possible precursor concentration to the nozzle at industrial scale production rates (1–5 kg/h). For a large scale reactor (up to 5 kg/h), the simulation results showed that the primary particle diameter can be controlled at ~20 nm, while the production rate was increased from 1 to 5 kg/h. Keeping the GLFR constant similar particle size can be obtained at fixed precursor concentration. The results also showed that the particle size can be reduced to ~15 nm by increasing GLFR from

1300 to 2100. For further reduction of cost and size of particles and to increase the process safety, the effect of oxidant/dispersion gas composition on the combustion of precursor solution and evolution of particles was investigated. The results showed that using air as dispersion gas would be able to increase the safety of the reactor since the maximum process temperature with air as oxidant was decreased by 21%. In addition, replacing oxygen with air led to smaller primary particle size (down to 12 nm) which was attributed to lower flame temperatures. A systematic investigation of suitable measures for PI in FSP synthesis of ZrO_2 nanoparticles was presented in this work. The quantitative simulation results can be used as a design guide to fulfil the fundamental aspects of PI in FSP process.

Acknowledgement

This work was supported by the European Community's Seventh Framework Programme under Grant no. CP-FP 228885-2.

Appendix A. Supplementary data

Supplementary data associated with this article can be found, in the online version, at http://dx.doi.org/10.1016/j.cep.2014.01.009.

References

[1] L. Mädler, H.K. Kammler, R. Mueller, S.E. Pratsinis, Controlled synthesis of nanostructured particles by flame spray pyrolysis, Journal of Aerosol Science 33 (2002) 369–389.
[2] K. Wegner, S.E. Pratsinis, Flame synthesis of nanoparticles, Chimica Oggi 22 (2004) 27–29.
[3] R. Mueller, R. Jossen, H.K. Kammler, S.E. Pratsinis, M.K. Akhtar, Growth of zirconia particles made by flame spray pyrolysis, AIChE Journal 50 (2004) 3085–3094.
[4] R. Mueller, R. Jossen, S.E. Pratsinis, M. Watson, M.K. Akhtar, Zirconia nanoparticles made in spray flames at high production rates, Journal of the American Ceramic Society 87 (2004) 197–202.
[5] A.J. Gröhn, S.E. Pratsinis, K. Wegner, Fluid-particle dynamics during combustion spray aerosol synthesis of ZrO_2, Chemical Engineering Journal 191 (2012) 491–502.
[6] H. Torabmostaedi, T. Zhang, P. Foot, S. Dembele, C. Fernandez, Process control for the synthesis of ZrO_2 nanoparticles using FSP at high production rate, Powder Technology 246 (2013) 419–433.
[7] L. Mädler, W.J. Stark, S.E. Pratsinis, Flame-made ceria nanoparticles, Journal of Materials Research 17 (2002) 1356–1362.
[8] L. Mädler, S.E. Pratsinis, Bismuth oxide nanoparticles by flame spray pyrolysis, Journal of the American Ceramic Society 85 (2002) 1713–1718.
[9] R. Mueller, L. Mädler, S.E. Pratsinis, Nanoparticle synthesis at high production rates by flame spray pyrolysis, Chemical Engineering Science 58 (2003) 1969–1976.
[10] M.C. Heine, S.E. Pratsinis, Droplet and particle dynamics during flame spray synthesis of nanoparticles, Industrial and Engineering Chemistry Research 44 (2005) 6222–6232.
[11] M.C. Heine, L. Mädler, R. Jossen, S.E. Pratsinis, Direct measurement of entrainment during nanoparticle synthesis in spray flames, Combustion and Flame 144 (2006) 809–820.
[12] M.J. Hounslow, R.L. Ryall, V.R. Marshall, A discretized population balance for nucleation, growth, and aggregation, AIChE Journal 34 (1988) 1821–1832.
[13] F.E. Kruis, K.A. Kusters, S.E. Pratsinis, B. Scarlett, A simple model for the evolution of the characteristics of aggregate particles undergoing coagulation and sintering, Aerosol Science and Technology 19 (1993) 514–526.
[14] Y. Xiong, S.E. Pratsinis, Formation of agglomerate particles by coagulation and sintering—Part I. A two-dimensional solution of the population balance equation, Journal of Aerosol Science 24 (1993) 283–300.
[15] G. Skillas, C. Becker, J. Vorholz, Simulation model deployment for particulate processes in an industrial environment, Chemical Engineering and Processing 45 (2006) 815–825.
[16] T. Johannessen, S.E. Pratsinis, H. Livbjerg, Computational analysis of coagulation and coalescence in the flame synthesis of titania particles, Powder Technology 118 (2001) 242–250.
[17] H. Mühlenweg, A. Gutsch, A. Schild, S.E. Pratsinis, Process simulation of gas-to-particle-synthesis via population balances: investigation of three models, Chemical Engineering Science 57 (2002) 2305–2322.
[18] A. Stankiewicz, J.A. Moulijn, Process intensification: transforming chemical engineering, Chemical Engineering Progress 96 (2000) 22–34.
[19] V. Parvulescu, S. Coman, P. Grange, V.I. Parvulescu, Preparation and characterization of sulfated zirconia catalysts obtained via various procedures, Applied Catalysis 176 (1999) 27–43.
[20] N. Miura, H. Kurosawa, M. Hasei, G. Lu, N. Yamazoe, Stabilized zirconia-based sensor using oxide electrode for detection of NO_x in high-temperature combustion-exhausts, Solid State Ionics 86–88 (Part 2) (1996) 1069–1073.
[21] Z. Mutasim, W. Brentnall, Thermal barrier coatings for industrial gas turbine applications: an industrial note, Journal of Thermal Spray Technology 6 (1997) 105–108.
[22] L. Grunberg, A.H. Nissan, Mixture law for viscosity, Nature 164 (1949) 799–800.
[23] M. Tamura, M. Kurata, On the viscosity of binary mixtures of liquids, Bulletin of Chemical Society of Japan 25 (1952) 32–38.
[24] R.K. Hind, E. McLaughlin, A.R. Ubbelohde, Structure and viscosity of liquids, Transactions of the Faraday Society 56 (1960) 328–330.
[25] T. Seto, A. Hirota, T. Fujimoto, M. Shimada, K. Okuyama, Sintering of polydisperse nanometer-sized agglomerates, Aerosol Science and Technology 27 (1997) 422–438.
[26] C.T. Crowe, Multiphase Flow Handbook, CRC Press, Boca Raton, 2006.
[27] L. Huimin, Science and Engineering of Droplets: Fundamentals and Applications, Noyes Publications/William Andrew Publishing, New York, 2000.
[28] C.C. Miesse, Correlation of experimental data on the disintegration of liquid jets, Industrial and Engineering Chemistry 47 (1955) 1690–1701.
[29] F.M. White, Fluid Mechanics, McGraw-Hill, New York, 1999.